07/70

# Rapid Solutions for Application Specific IGBT Module Design

D.R.Newcombe [†],
Dynex Semiconductor Ltd., Doddington Road, Lincoln, England

Chris Bailey* and Hua Lu
School of Computing and Mathematical Sciences, Greenwich University
30 Park Rod, London SE9 3SN

[†] Email: david_newcombe@dynexsemi.com
* Email : c.bailey@gre.ac.uk

## ABSTRACT

The electric car, the all electric aircraft and requirements for renewable energy are prime examples of potential technologies needing to be addressed in the world problem of global warming/carbon emission etc.
Power electronics are fundamental for the underpinning of these technologies and with the diverse requirements for electrical configurations and the range of environmental conditions, time to market is paramount for module manufacturers and systems designers alike.
This paper presents a 'virtual' design methodology together with theoretical and experimental results that demonstrate enhanced product design with improved reliability, performance and cost value within competitive time scales.

## 1. INTRODUCTION

Manufacturing prototypes, for copper bus barring and mimic-plastic mouldings is now a mature procedure for early electrical assessment. However a significant delay in the time to market process occurs at the qualification stage, especially in some applications where a very large temperature cycling regime is encountered.
A project, being part-funded by the UK Government, is developing 'virtual' reliability models to simulate operational wear out and failure mechanisms in electronic power modules.
This paper will demonstrate the methodology used during the design phase to ensure that reliability and fit for purpose issues are addressed. Physics of failure (POF) analyses for the various package technologies will be discussed together with a more detailed study of the substrate to base plate solder interface.

Fig. 1 shows a typical 800A IGBT plastic module used in a rail traction application.

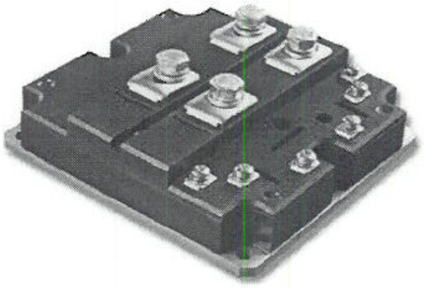

Figure 1. IGBT Module for Rail Traction

Fig. 2 is an internal schematic of the above module construction indicating the area under consideration.
This paper will present new work, which demonstrates the strategy for producing high confidence design capability using the POF approach.

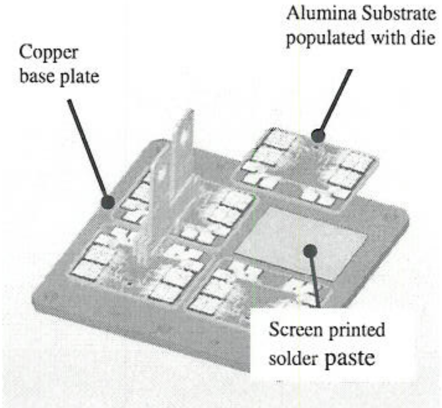

Figure 2. Solid model of subassembly

## 2. METHODOLOGY

### 2.1 Original Approach

The original approach for demonstrating fit for purpose for a given application is simply to perform temperature cycling tests according to a MIL STD condition. Fig. 3 is an extract from the MIL STD 888F-1010.8 for temperature cycling using a chamber to chamber temperature regime.

| | Time at temp | A | B | C |
|---|---|---|---|---|
| Cold | >10mins | -55°C | -55°C | -65°C |
| Hot | >10mins | +85°C | 125°C | 150°C |
| Cycles | | 10 | 10 | 10 |

Figure 3. MIL STD Temperature Cycling

This test methodology is still valid i.e. slow heating and cooling with rapid component transfer. However these MIL standards were derived many years ago for small discrete semiconductors and hence bear little relevance to the large volume hermetic or plastic IGBT packages of the modern era. This discrepancy arises due to the high temperature gradation between the semiconductor die and the heat sink. To ensure customer confidence, it becomes increasingly important that the cycling regime during a qualification accurately aligns to the application that the cycles are meant to relate to.

With the advent of the All-Electric Aircraft, temperature cycling of up to 20,000 cycles may be required for some applications: For example, based on 2 hours at each temperature extreme this would result in qualification times of approximately 20 years! This shows the need for a deeper understanding of accelerated failure mechanisms, especially with the new Sn/Ag/Cu solders (with even higher temperatures envisaged).

### 2.2 Coffin-Manson Approach

Present day methodology would dictate high stress testing in order to produce life curves which can be curve fitted with a Coffin-Manson equation of the form:

$$N_f = c_1 \Delta T^{c_2} \qquad \text{Equation (1)}$$

where $N_f$ is the number of cycles to failure, $\Delta T$ is the temperature range, $c_1$ and $c_2$ are empirical constants that are dependent on the device design.

This paper focuses on the substrate to base plate solder shown in Fig. 2.

Acceleration curves are produced for a range of $\Delta T$ and the number of cycles to failure recorded. The failure criteria, during the qualification test, is identified as an increase of 20% in the thermal resistance, however it must be appreciated that the degradation of thermal resistance will be totally dependent on the position of die on the substrate. Therefore for the purpose of this paper, failure criteria is seen as a 20% reduction in bonded area. Figs 4 and 5 below show a typical failure as measured by Scanning Acoustic Microscopy and the acceleration curve for the solder in question.

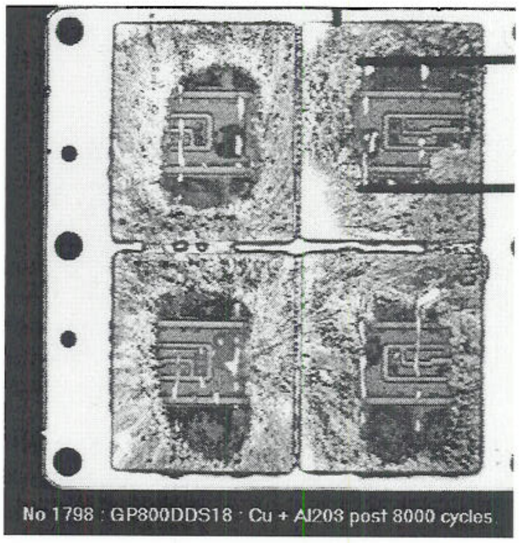

Figure 4. Scanning Acoustic Micrograph of solder bond (8000 cycles wth delta T of 80°C)

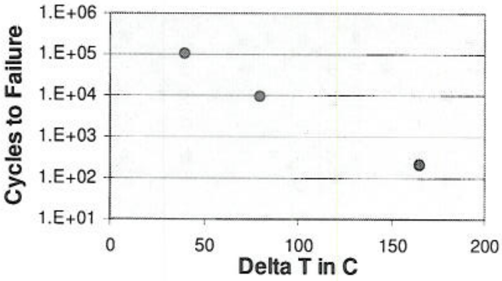

Figure 5. Acceleration Curve for temperature cycling of IGBT substrate solder.

A typical example would be for a rail traction application. From the load profile given by the customer, Finite Element Analysis (FEA) would be typically used to quantify the delta T of the technologies under consideration.

By normalising each of the temperature excursions to one equivalent value of delta T a single figure of merit can be used and the wear out life quantified at that condition.

The Coffin-Manson technique is a perfectly acceptable approach for a specific structure that has been fully characterised. However if there is then a need to change one of the process parameters such as solder bond line thickness and area, the acceleration trials need to be repeated.

## 2.3 Physics of Failure Approach

POF analysis is a science-based approach to reliability prediction. It combines laboratory test data with recognised failure models and hence has the ability to predict the lifetime of electronics component/systems under a variety of specified loading conditions. The methodology for POF approach is summarised in Fig. 6 below.

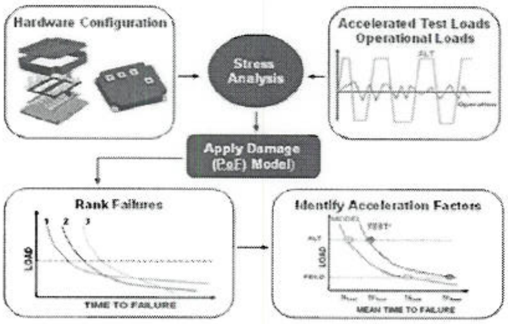

Figure 6. Physics of failure approach to reliability prediction.

Importantly, when POF is used, design optimisation simulations can be developed within the process constraints of the manufacture. This methodology is outlined in Fig. 7.

.

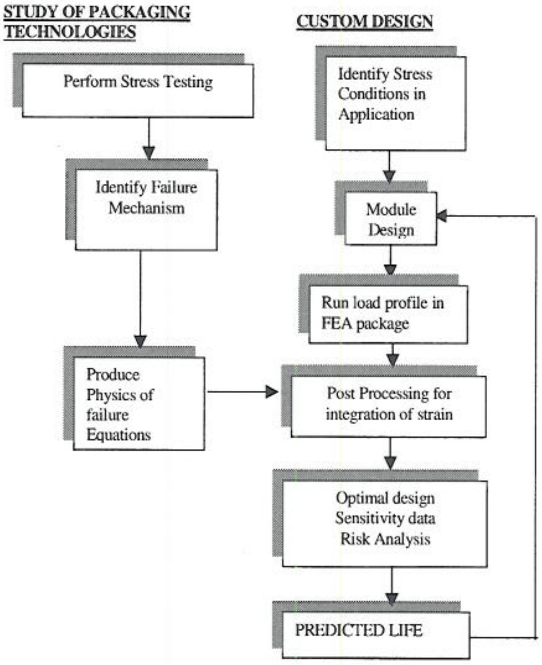

Figure 7. Physics of failure approach for design optimization.

The most critical step in this process is to accurately define the POF equations that allow predicted life expectancy.

Unlike Coffin–Manson, POF must identify and focus on the various failure mechanisms that can occur in a generic design.

As an example, in this work the lifetimes of substrate mount-down solder interconnects are predicted using FE simulation for a range of solder thickness designs. The solder alloy is assumed to be SnPb and its properties can be found in [ref. 1]. From simulation, the plastic strain and plastic work in the joint are obtained as a function of time. The plastic strain per cycle is then derived.

In fact, there are two types of solder fatigue models namely, plastic work density and plastic strain range.

In the former, the plastic work energy density per thermal cycle acts as a damage indicator whereas in the latter the accumulated strain per cycle is used. In this paper, the plastic strain approach has been adopted using the following equation.

$$\frac{dL}{dN} = 5.7 \times 10^{-3} \left( \Delta \varepsilon_p \right)^{0.7376} \qquad \text{Equation (2)}$$

where $\Delta \varepsilon_p$ is the accumulated plastic strain per cycle, *L* is the crack length in millimetres, *N* is the number of cycles [ref. 2].

Eutectic Sn/b solder was used since to the authors' knowledge there is no equivalent rate equation for SnAg solder in the literature at present.

Although equation (2) is also in the form of a Coffin Manson type equation, it is fundamentally different to equation (1).

In equation (1), the temperature excursion $\Delta T$ is only one of the load environment parameters and is not directly related to crack propagation or any specific failure mechanism. Therefore, for any change in design, the constants in equation (1) have to be modified. In equation (2) however, $\Delta\varepsilon_p$ has been proved by experiment to be correlated to crack propagation rate in the solder and its value is determined by all the design and environmental parameters.

For a given cracked area at the point of failure, the lifetime (number of cycles to failure) for thermal-mechanical loads with constant amplitude can be calculated using the crack propagation rate equation and the cracked area value. For spectrum loading conditions where several loads with different amplitudes are combined, component lifetime can be predicted using Miner's linear cumulative damage rule [ref. 3].

This rule states that the device will fail if the following condition is met:

$$\sum_{i=1}^{N_{tot}} \frac{n_i}{N_i} = 1 \qquad \text{Equation (3)}$$

where $N_i$ is the lifetime for the $i$th load profile, $n_i$ is the number of cycles the device has been exposed to the $i$th load profile, and $N_{tot}$ is the total number of load profiles.

From Equation 3, the following equations can be derived and the lifetime in years, $Y_f$, can be calculated.

$$AF_i = \frac{N_{ref}}{N_i},$$

$$C_i = AF_i \times m_i, \qquad \text{Equation (4)}$$

$$Y_f = \frac{N_{ref}}{365\sum_{i=1}^{N_{tot}} C_i}.$$

where $N_{ref}$ is the reference number of cycles to failure, subscript $i$ represents the $i$th load profile, $AF_i$ is the acceleration factor, $C_i$ is the normalised cycles per day, $m_i$ is the number of cycles per day. The reference load profile can be any one of the load profiles for which the life times have been calculated.

Fig. 8 shows a cross section through the module structure in Fig. 2. The elastic properties of the materials are listed in Fig. 9.

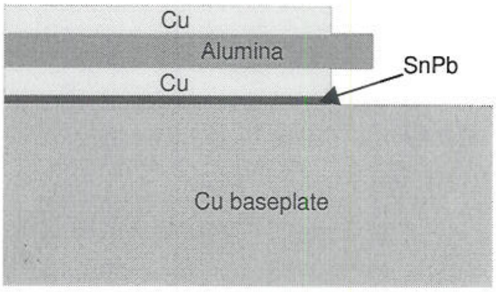

Figure 8. Substrate mount-down interconnect model.

| | Alumina | Cu | SnPb |
|---|---|---|---|
| E(GPa) | 270 | 115 | 36.68-0.156T |
| ν | 0.22 | 0.31 | 0.4 |
| CTE(ppm/°C) | 7.4 | 17.3 | 24 |

Figure 9: Material properties used for the finite element analysis. The temperature is in ℃.

Computer modelling methods allow parameterised module data to define the range of design parameters to be investigated. The process can be made more efficient by incorporating design of experiment (DOE) methods to generate response surfaces, which approximate the solution. The effects of parameter tolerance uncertainty can also be assessed using Monte-Carlo techniques. Overall these modelling procedures produce an optimal design for the module, and a statistical indication of the influence on material and process tolerances on performance.

## 3. RESULTS

### 3.1 Design Requirement

a. *Customer Specification*

As previously stated, load profiles, provided by the customer, are fed into a FEA simulator in order to quantify the delta temperatures seen at various locations within the module package. Figs. 10a and 10b below show the temperature response at the substrate to base plate solder interface for two differing rail traction applications.

| Status | Low Temp | High Temp | Delta T | Cycles / day |
|---|---|---|---|---|
| Shed stops | -40°C | +80°C | 120°C | 1 |
| Station Stops | +80°C | +100°C | 20°C | 1080 |
| Cruise | +80°C | +81°C | 1°C | 6E6 |

Figure 10 a. Mass Transit: Base plate solder response

| Status | Low Temp | High Temp | Delta T | Cycles / day |
|---|---|---|---|---|
| Shed stops | -40°C | +80°C | 120°C | 1 |
| Station Stops | +80°C | +100°C | 20°C | 20 |
| Speed Control | +80°C | +85°C | 5°C | 3240 |
| Cruise | +80°C | +81°C | 1°C | 6E6 |

Figure 10 b. High Speed: Baseplate solder response.

*b. Process Parameters*

Four cases of the substrate mount-down solder interconnect are considered in this work. The parameters for these variants are listed in Fig. 11.

|  | Solder thickness (mm) | Solder width (mm) |
|---|---|---|
| Case 1 | 0.1 | 56 |
| Case 2 | 0.2 | 56 |
| Case 3 | 0.5 | 56 |
| Case 4 | 1.0 | 56 |

Figure 11. Table of process variants under consideration.

### 3.2 Calculation strategies

a. *Coffin Manson Calculation*

As previously identified, this is the default build standard and in this case is 56x50mm substrates bonded to a copper base plate using 100 micron thick solder paste.

Fig. 12 below curve fits the Coffin Manson equation to Fig. 5.

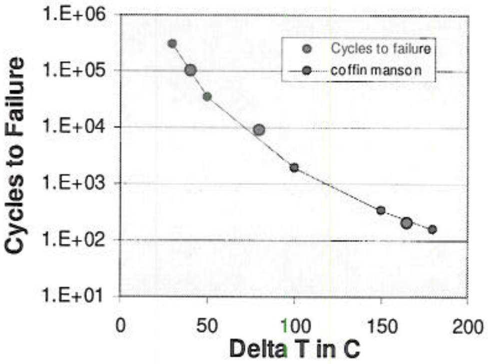

Figure 12. Coffin Manson curve fit to the lifetime data.

For each of the temperature stress profiles identified in Figs. 10a and 10b, an acceleration factor relative to a reference stress profile can be calculated and the values normalised to obtain a life prediction. These results are tabulated in Fig. 13.

| Application | Status | Accel. Factor $AF_i$ | Norm. cycles/day $C_i$ |
|---|---|---|---|
| Mass Transit | Shed Stops | 5.49 | 5.49 |
|  | Station Stops | 2.96E-3 | 3.2 |
|  | Cruising | 1.02E-8 | 6.12E-2 |
| **Calculated Life $Y_f$** |  | **2.8 Years** |  |
| High Speed | Shed Stops | 5.49 | 5.49 |
|  | Station Stops | 2.96E-3 | 5.92E-2 |
|  | Speed Control | 8.76E-6 | 2.84E-2 |
|  | Cruising | 1.02E-8 | 5.49 |
| **Calculated Life $Y_f$** |  | **4.4 Years** |  |

Figure 13. Acceleration Factors for each Stress Condition

Note it is because of this low life prediction that Rail Traction modules use AlN substrates combined with Al–SiC metal matrix composites to reduce CTE mismatch and increase life to the required 30 years.

*b. Computer Modelling Results*

For each load profile and geometry listed in Figs. 10a, 10b and 11, a simulation is carried over an arbitrary three cycles of time. For example, for the shed stop temperature cycle it is assumed that each cycle lasts for one hour so the simulation will be carried over three hours. Fig. 14 shows a snapshot of stress distribution in the substrate mount-down during cyclic temperature loading. The deformation has been exaggerated by 20 times in this figure.

Figure 14. Stress and deformation when the substrate mount-down device cools from 80°C to -40°C.

Fig. 15 shows the accumulated plastic strain at the end of the simulation time. The plastic strain is the highest at the substrate-solder interface and this location is where a crack is most likely to initiate. Fig. 16 shows how this plastic strain changes during these three cycles of loading. The accumulated plastic strain over one cycle $\Delta\varepsilon_p$ is different from that in another cycle because of the transient effect at the beginning of the simulation run. This difference will become smaller and smaller after a few cycles when a steady state is reached. In this work, the $\Delta\varepsilon_p$ value over the third cycle will be used for crack propagation rate and lifetime calculation to make sure the steady state has been reached and the transient effect is negligible.

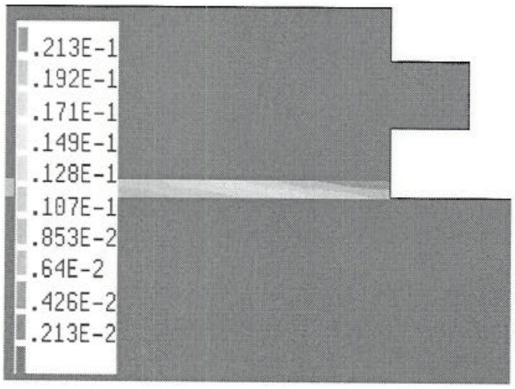

Figure 15. Accumulated plastic strain at the end of three thermal-mechanical cycles.

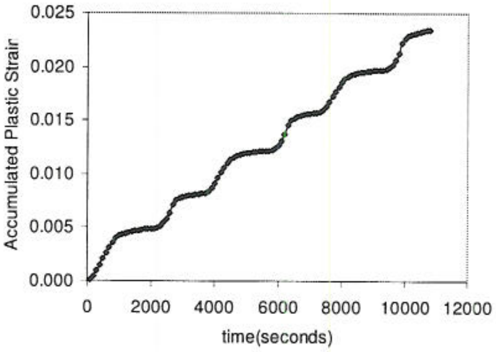

Figure 16. The accumulated plastic strain as a function of time.

Having calculated the crack propagation rates, lifetimes can be estimated by dividing the failure crack length by the propagation rates. For the 56 mm substrate the failure crack length is about 4 mm and for the 28 mm substrate the failure crack length is about 1.9 mm. The calculated lifetime in numbers of cycles to failure for the four different load profiles are summarised in Fig. 17.

| Case | Cruising | station | shed | speed control |
|---|---|---|---|---|
| 1 | 1.9E+11 | 1.3E+05 | 2.5E+04 | 1.6E+07 |
| 2 | 2.3E+11 | 1.6E+05 | 3.1E+04 | 2.0E+07 |
| 3 | 2.9E+11 | 2.0E+05 | 3.5E+04 | 2.5E+07 |
| 4 | 3.3E+11 | 2.2E+05 | 3.6E+04 | 2.8E+07 |

Figure 17. The predicted number of cycles to failure.

The lifetime in number of years for the solder interconnect under a combined spectrum load can be calculated using the lifetimes for each simple cyclic load and Miner's rule-Equation (4). The results are summarised in Fig. 18.

| | Lifetime (Years) | |
|---|---|---|
| model | Mass transit | High speed |
| 1 | 0.34 | 6.53 |
| 2 | 0.41 | 7.90 |
| 3 | 0.49 | 9.69 |
| 4 | 0.54 | 10.67 |

Figure 18: Predicted service life in years.

These results show that the mass transit and high speed applications have very different lifetime for SnPb solder interconnect. On further analysis, this is mainly caused by the difference in the number of station stops for the two applications.

The lifetimes predicted for SnPb solder joint are quite different from what have been observed for the SnAg as shown in Fig. 5. However, the methodology that has been presented here shows that it is possible to quickly predict changes in lifetime as geometry is altered. This is obviously not possible using the traditional Coffin Manson experimentation.

c Summary of Results

The build standard of modules, currently in manufacture, uses eutectic Sn/Ag solder for the joint between the alumina substrate and copper base plate and the experimental work to derive acceleration factors uses this configuration. As a crack prediction model for the silver /tin system is not yet available, the computer model results are derived from Pb/Sn studies: A direct comparison is not therefore possible.

Fig. 18 summarises the results of life prediction and Fig. 19 is a graph showing the effect of solder thickness on life for the high speed case.

| Solder thickness | Coffin Manson | Physics of Failure |
|---|---|---|
| | **Mass Transit** | |
| 100 μm | 2.8 years | 0.34 years |
| 200 μm | Unable to predict | 0.41 years |
| 500 μm | Unable to predict | 0.49 years |
| 1000 μm | Unable to predict | 0.54years |
| | **High Speed** | |
| 100 μm | 4.4 years | 6.53 years |
| 200 μm | Unable to predict | 7.90 years |
| 500 μm | Unable to predict | 9.69 years |
| 1000 μm | Unable to predict | 10.67years |

Figure 18 Summary of life prediction

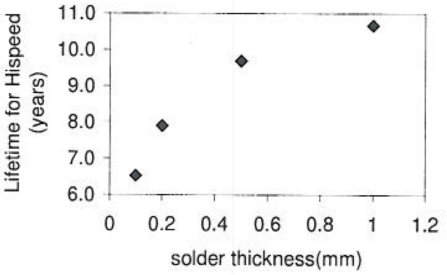

Figure 19 Effect of solder thickness on life (high speed case)

## 4. CONCLUSION

A traditional Coffin-Manson method has been used to predict lifetimes of substrate mount-down solder interconnect for two module traction applications. This method cannot be used efficiently for design optimization purpose because it is only suitable for a specific device construction. The physics of failure method, however, can be used to calculate life expectancy when the geometry and/or load profiles have been altered. This method can be integrated with optimization and statistical tolerancing tools to simulate designs with a high degree of confidence. This paper has demonstrated such strategy using a model with eutectic Pb/Sn solder interconnects.

Future work will:

- Develop failure models for Sn/Ag and SAC solders and novel nano bonding materials
- Extend the POF models to include extra stress modes ie temperature cycling plus vibration
- Extend the POF models to include real time dependent loading e.g. creep relaxation during shed stop will be very different from that encountered during a station stop.

.

## ACKNOWLEDGEMENTS

The authors wish to thank the following Partners of the MPM Project for their contribution and support to this paper:
A.T.Plumpton (Dynex Semiconductors)
S.R.Jones and R.Rhodes (Semelab)
G.Ferry and M.Woodhouse (Areva –TD Ltd)
R.Young (Faraday Advance)
L.Allen (Raytheon)
M.Holme (Goodrich)., I.Jordison (SR Drives)
Tim Tilford, (Greenwich University)

The Partners also wish to thank the UK Department of Trade and Industry for their financial support of the project.

## REFERENCES

Ref. [1.] J.H. Lau (editor), *Ball Grid Array Technology*, McGraw-Hill (1995), p.396

Ref. [2] S. Déplanque, W. Nüchter, B. Wunderle, R. Schacht, B. Michel, 'Lifetime Prediction of SnPb and SnAgCu Solder Joints of Chips on Copper Substrate Based on Crack Propagation FE-Analysis', *Proceedings of Eurosime 2006*, pp.243-250 (2006)

Ref. [3] S. Suresh, *Fatigue of Materials*, Cambridge University Press (1991), p.133